UC Davis

UC Davis Previously Published Works

Title

HIPPO–Integrin-linked Kinase Cross-Talk Controls Self-Sustaining Proliferation and Survival in Pulmonary Hypertension

Permalink

https://escholarship.org/uc/item/9500t4dn

Journal

American Journal of Respiratory and Critical Care Medicine, 194(7)

ISSN

1073-449X

Authors

Kudryashova, Tatiana V
Goncharov, Dmitry A
Pena, Andressa
et al.

Publication Date

2016-10-01

DOI

10.1164/rccm.201510-2003oc

Peer reviewed

eScholarship.org Powered by the California Digital Library
University of California

ORIGINAL ARTICLE

HIPPO–Integrin-linked Kinase Cross-Talk Controls Self-Sustaining Proliferation and Survival in Pulmonary Hypertension

Tatiana V. Kudryashova[1]*, Dmitry A. Goncharov[1]*, Andressa Pena[1], Neil Kelly[2], Rebecca Vanderpool[1], Jeff Baust[1], Ahasanul Kobir[1], William Shufesky[3], Ana L. Mora[1,2], Adrian E. Morelli[3], Jing Zhao[2], Kaori Ihida-Stansbury[4,5], Baojun Chang[1,2], Horace DeLisser[5,6], Rubin M. Tuder[7], Steven M. Kawut[5,8], Herman H. W. Silljé[9], Steven Shapiro[2], Yutong Zhao[1,2], and Elena A. Goncharova[1,2]

[1]Heart, Lung, Blood and Vascular Medicine Institute, [2]Department of Medicine, and [3]Department of Surgery and Immunology, University of Pittsburgh School of Medicine, Pittsburgh, Pennsylvania; [4]Department of Pathology and Laboratory Medicine, [5]Pulmonary Vascular Disease Program, [6]Department of Medicine, and [8]Center for Clinical Epidemiology and Biostatistics, University of Pennsylvania Perelman School of Medicine, Philadelphia, Pennsylvania; [7]Division of Pulmonary Sciences and Critical Care Medicine, University of Colorado Denver, Aurora, Colorado; and [9]Department of Cardiology, University Medical Center Groningen, University of Groningen, Groningen, the Netherlands

ORCID IDs: 0000-0002-2843-5554 (T.V.K.); 0000-0001-7118-6752 (E.A.G.).

Abstract

Rationale: Enhanced proliferation and impaired apoptosis of pulmonary arterial vascular smooth muscle cells (PAVSMCs) are key pathophysiologic components of pulmonary vascular remodeling in pulmonary arterial hypertension (PAH).

Objectives: To determine the role and therapeutic relevance of HIPPO signaling in PAVSMC proliferation/apoptosis imbalance in PAH.

Methods: Primary distal PAVSMCs, lung tissue sections from unused donor (control) and idiopathic PAH lungs, and rat and mouse models of SU5416/hypoxia-induced pulmonary hypertension (PH) were used. Immunohistochemical, immunocytochemical, and immunoblot analyses and transfection, infection, DNA synthesis, apoptosis, migration, cell count, and protein activity assays were performed in this study.

Measurements and Main Results: Immunohistochemical and immunoblot analyses demonstrated that the HIPPO central component large tumor suppressor 1 (LATS1) is inactivated in small remodeled pulmonary arteries (PAs) and distal PAVSMCs in idiopathic PAH. Molecular- and pharmacology-based analyses revealed that LATS1 inactivation and consequent up-regulation of its reciprocal effector Yes-associated protein (Yap) were required for activation of mammalian target of rapamycin (mTOR)-Akt, accumulation of HIF1α, Notch3 intracellular domain and β-catenin, deficiency of proapoptotic Bim, increased proliferation, and survival of human PAH PAVSMCs. LATS1 inactivation and up-regulation of Yap increased production and secretion of fibronectin that up-regulated integrin-linked kinase 1 (ILK1). ILK1 supported LATS1 inactivation, and its inhibition reactivated LATS1, down-regulated Yap, suppressed proliferation, and promoted apoptosis in PAH, but not control PAVSMCs. PAVSM in small remodeled PAs from rats and mice with SU5416/hypoxia-induced PH showed down-regulation of LATS1 and overexpression of ILK1. Treatment of mice with selective ILK inhibitor Cpd22 at Days 22–35 of SU5416/hypoxia exposure restored LATS1 signaling and reduced established pulmonary vascular remodeling and PH.

Conclusions: These data report inactivation of HIPPO/LATS1, self-supported via Yap–fibronectin–ILK1 signaling loop, as a novel mechanism of self-sustaining proliferation and apoptosis resistance of PAVSMCs in PAH and suggest a new potential target for therapeutic intervention.

Keywords: HIPPO/LATS1; ILK; PAH; vascular smooth muscle; proliferation/apoptosis imbalance

(Received in original form October 14, 2015; accepted in final form March 29, 2016)

*These authors contributed equally.

Supported by National Institutes of Health/NHLBI grants R01HL113178 (E.A.G.), R01HL130261 (E.A.G.), 5P01HL103455-05 (A.L.M.), and K24 HL103844 (S.M.K.). The Pulmonary Hypertension Breakthrough Initiative is supported by National Institutes of Health/NHLBI grant R24HL123767.

Authors Contributions: Conception and design, D.A.G., R.M.T., and E.A.G. Experimental work, analysis, and interpretation, T.V.K., D.A.G., A.P., N.K., A.K., B.C., W.S., A.L.M., A.E.M., R.V., J.B., K.I.-S., R.M.T., J.Z., H.H.W.S., Y.Z., and E.A.G. Drafting the manuscript and intellectual content, D.A.G., N.K., K.I.-S., H.D., R.M.T., S.M.K., H.H.W.S., S.S., Y.Z., and E.A.G.

Correspondence and requests for reprints should be addressed to Elena A. Goncharova, Ph.D., BST E1259, 200 Lothrop Street, Pittsburgh, PA 15261. E-mail: eag59@pitt.edu

This article has an online supplement, which is accessible from this issue's table of contents at www.atsjournals.org

Am J Respir Crit Care Med Vol 194, Iss 7, pp 866–877, Oct 1, 2016
Copyright © 2016 by the American Thoracic Society
Originally Published in Press as DOI: 10.1164/rccm.201510-2003OC on April 27, 2016
Internet address: www.atsjournals.org

At a Glance Commentary

Scientific Knowledge on the Subject: Increased proliferation and impaired apoptosis of pulmonary arterial vascular smooth muscle cells (PAVSMCs) are important pathophysiologic components of pulmonary arterial hypertension (PAH), the understanding of which is crucial for identifying new molecular targets to treat this incurable disease.

What This Study Adds to the Field: This study reports inactivation of HIPPO/LATS1 as a novel mechanism supporting the proliferative apoptosis-resistant PAH PAVSMC phenotype, pulmonary vascular remodeling, and pulmonary hypertension. Our data describe a novel self-supported pathologic loop between LATS1 and integrin-linked kinase 1 as an important regulator of self-sustaining proliferation and survival of PAVSMCs in PAH and provide a new potential target pathway for therapeutic intervention.

Pulmonary arterial hypertension (PAH) is a progressive fatal disease with a high mortality rate (1). PAH manifests by vasoconstriction and remodeling of small pulmonary arteries (PAs) leading to increased PA pressure, elevated right ventricular (RV) afterload, and death (2). Although marked progress had been made in a treatment of PAH, available therapies fail to reverse established pulmonary vascular remodeling or prevent disease progression in most patients (3, 4), and new molecular targets for development of remodeling-focused therapeutics are urgently needed.

Increased proliferation and impaired apoptosis of vascular cells in small PAs are key components of pulmonary vascular remodeling in PAH (3, 5). Distal pulmonary arterial vascular smooth muscle cells (PAVSMCs) in PAH undergo complex signaling reprogramming resulting in loss of growth suppressors, persistent activation of proproliferative/prosurvival pathways, and acquisition of unique disease-specific phenotype with intrinsic proliferative/prosurvival potential (5–7). The complexity of molecular abnormalities led us to hypothesize that signaling components shared by known pathologic pathways and functionally linked to PAH might represent attractive therapeutic targets to selectively reduce PAH PAVSMC proliferation, promote apoptosis, and reverse pulmonary vascular remodeling.

The HIPPO signaling pathway is a master-regulator of proliferation/apoptosis balance that prevents organ overgrowth by restricting cell proliferation and inducing cell differentiation or apoptosis (8). HIPPO is comprised of Ste20-like proteinkinases (MST) 1/2 that activate large tumor suppressors (LATS) 1/2 by phosphorylation at T1079 (9). Major reciprocal effectors of HIPPO are transcriptional coactivators Yap/Taz, which are inhibited by LATS-dependent phosphorylation, instigating their degradation (8). Yap/Taz promote proliferation and survival via regulating other transcriptional factors, and their up-regulation has recently been reported as an important component of PAH progression (10). HIPPO is regulated by multiple inputs (mitogens, extracellular matrix [ECM] composition, and stiffness) (8), all of which are implicated in PAH pathogenesis (2, 11, 12), and is scored as one of the most highly related pathways to PAH by data-mining approaches (13), suggesting its possible role in regulating PAVSMC proliferation and survival in PAH.

In the present study, we report a novel role for the HIPPO central component LATS1 as an important regulator of proliferation/apoptosis imbalance in human PAH PAVSMCs, present a novel mechanism supporting self-sustaining proliferative/apoptosis-resistant PAH PAVSMC phenotype, and provide a new potential target pathway for therapeutic intervention.

Methods

The online supplement provides more detailed information.

Human Tissues and Cell Cultures

Unused donor (control) and idiopathic PAH lung sections were provided by the Pulmonary Hypertension Breakthrough Initiative. Primary distal PAVSMCs from different subjects were provided by Pulmonary Hypertension Breakthrough Initiative and the University of Pittsburgh Vascular Medicine Institute Cell Processing Core under approved protocols. Cells isolation, characterization, and maintenance were performed under Pulmonary Hypertension Breakthrough Initiative protocols as described elsewhere (5). All experiments were repeated on primary (3–8 passage) PAVSMCs from a minimum of three subjects. Before experiments, cells were incubated for 24–48 hours in basal media with 0.1% bovine serum albumin.

Immunohistochemical, Immunocytochemical, and Immunoblot Analyses and Transfection, Infection, DNA Synthesis, Apoptosis, Migration, and Cell Count Assays

These were performed as described (5, 14, 15). siRNAs and shRNAs were purchased from Dharmacon (Lafayette, CO) and Origen (Rockville, MD). Wild-type (WT), T1079A, and kinase-dead (KD) LATS1 construct design is described Figure E1 in the online supplement (9). The primer design and site-directed mutagenesis to generate LATS1 T1079D were performed according to the manufacturer's instructions (Agilent Technologies, Santa Clara, CA) (*see* Figure E2). Softwell hydrogel-coated plates were purchased from Matrigen (Brea, CA).

Activity Assays

For Yap/Taz activity assay, cells were cotransfected with Yap/Taz-responsive synthetic TEAD promoter 8 × GTIIC-luc (16) (Addgene, Cambridge, MA) and control pGL4 *Renilla* hRluc reporter (Promega, Madison, WI). An 8 × GTIIC-luc induction was counted as firefly/sea pansy luciferase ratio. Wnt/β-catenin and HIF1α activation assays were performed using Wnt/β-Catenin TF Activation Profiling Plate Array (Signosis, Santa Clara, CA) and TransAM HIF-1 (Active Motif, Carlsbad, CA) according to manufacturers' protocols.

Animals

All animal procedures were performed under the protocols approved by the University of Pittsburgh Animal Care and Use Committee. Six- to-eight-week-old male Sprague-Dawley rats (Charles River Laboratories, Wilmington, MA) received SU5416 injection (20 mg/kg, subcutaneously) and maintained for 3 weeks under chronic hypoxia (10% O_2), and for 5 weeks under normoxia (17, 18).

Six- to-eight-week-old male C57BL/6J mice (Jackson Laboratories, Bar Harbor, ME) were exposed to hypoxia (10% O_2) up to 35 days; SU5416 (20 mg/kg, subcutaneously) injections were performed at Days 0, 7, and 14. Treatment with Cpd22 (20 mg/kg, intraperitoneally 5 d/wk) (EMD Millipore, Billerica, MA) or vehicle was performed at Days 22–35. Negative control subjects included normoxia-maintained male age-matched animals (5, 14). Hemodynamic and histochemical analyses were performed as described (5, 19). Blinded analysis of small PAs (25–150 μm outer diameter) was performed as described (5, 20). The Fulton index was calculated as RV/(left ventricle [LV] + septum) weight ratio.

Data Analyses

Immunoblots, DNA synthesis, and apoptosis assays were analyzed using ImageJ (NIH, Bethesda, MD) and StatView (SAS Institute, Cary, NC) software, and hemodynamic and morphometric data using Indus Instruments (Webster, TX), IOX2 (Emka Technologies, Falls Church, VA), Emka (Emka Technologies), Matlab (MathWorks, Natick, MA), and MetaMorph (Nashville, TN). Statistical comparisons between two groups were performed by the Mann–Whitney *U* test. Statistical significance was defined as *P* less than or equal to 0.05.

Results

HIPPO/LATS1 Is Inactivated in Distal PAVSM from Subjects with PAH That Is Required for Increased Proliferation and Survival

Histochemical analysis revealed that smooth muscle α-actin (SMA)-positive areas of small (50–150 μM) remodeled, but not fully obliterated PAs from subjects with idiopathic PAH had marked reduction of active T1079-phosphorylated LATS1 and increased proliferation (detected by proliferating cell nuclear antigen [PCNA]) compared with control subjects (Figure 1A) suggesting the link between decreased P-LATS1 levels and VSMC remodeling *in vivo*. Primary distal PAVSMCs from patients with idiopathic PAH had P-T1079 LATS1 deficiency and significantly higher proliferation rates compared with control subjects (Figures 1B–1D). Transfection of human PAH PAVSMCs with construct encoding myc-tagged human LATS1 with

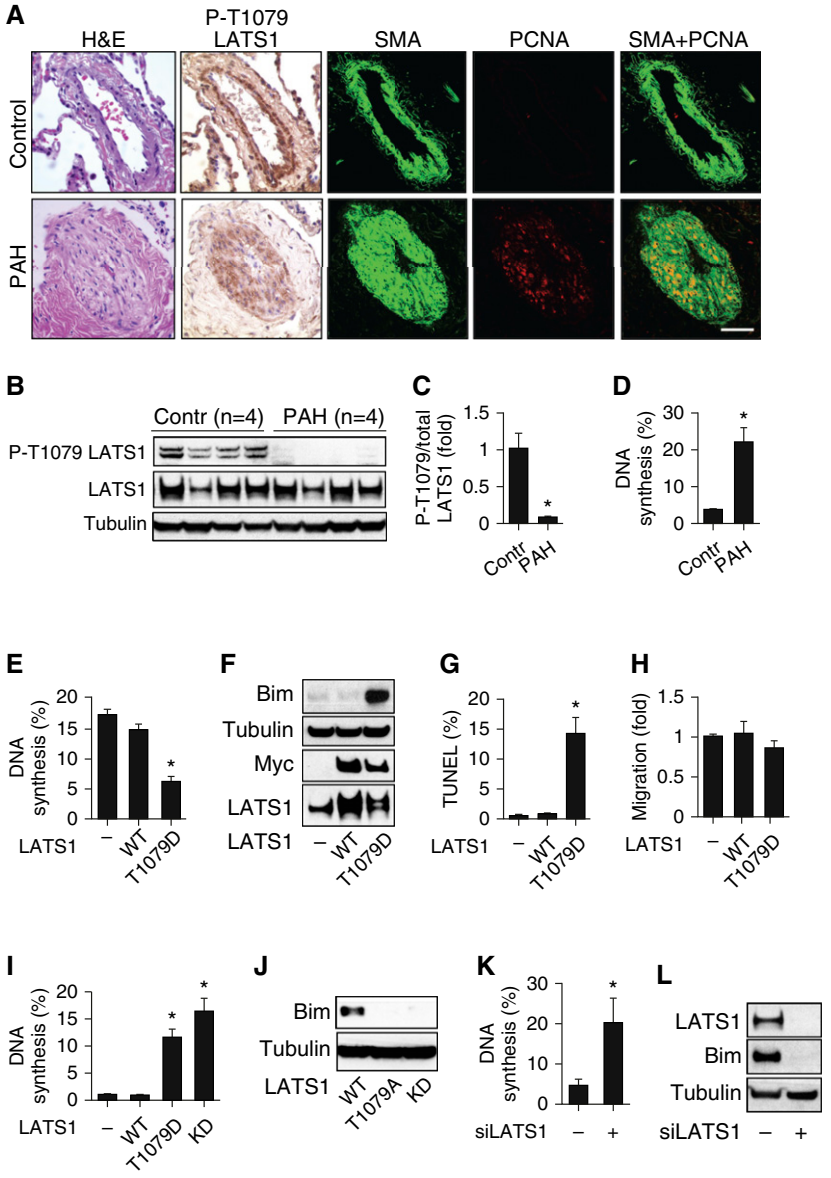

Figure 1. HIPPO/large tumor suppressor 1 (LATS1) is inactivated in pulmonary arterial vascular smooth muscle cells in human pulmonary arterial hypertension (PAH) that is required for increased proliferation and impaired apoptosis. (*A*) Histochemical analysis of human lung tissues. *Left to right*: hematoxylin and eosin (H&E) staining; P-T1079 LATS1 (*brown*); smooth muscle α-actin (SMA) (*green*); proliferating cell nuclear antigen (PCNA) (*red*); PCNA (*red*) + SMA (*green*) merge. Images are representative of three control subjects and three subjects with idiopathic PAH; minimum of 10 PA/subject. *Scale bar* = 50 μm. (*B–D*) Pulmonary arterial vascular smooth muscle cells from four idiopathic PAH and four control (Contr) subjects were subjected to immunoblot (*B* and *C*) or DNA synthesis (bromodeoxyuridine [BrdU] incorporation assay) (*D*) analyses. (*B*) Two bands = two alternatively spliced human LATS1 isoforms (50). (*C* and *D*) Data are P/total LATS1 ratio; folds to control (*C*) and percentage of BrdU-positive cells per total number of cells (*D*). Data are means ± SE; n = 4 subjects/group; $P < 0.05$ by Mann–Whitney *U* test. (*E–L*) Cells were transfected with indicated mammalian vectors or empty plasmid (−) (*E–J*) or small interfering RNA (siRNA) LATS1 and control siRNA GLO (−) (*K* and *L*) for 48 hours followed by DNA synthesis (BrdU) (*E*, *I*, and *K*), immunoblot (*F*, *J*, and *L*), apoptosis (terminal deoxynucleotidyl transferase dUTP nick end labeling [TUNEL]) (*G*), and migration (Boyden chamber assay) (*H*) analyses. (*F*, *J*, and *L*) Representative immunoblots from three (*F* and *J*) and four (*L*) subjects per group (*see* Figure E3 for statistical analysis). Data represent percentage of BrdU- (*E*, *I*, and *K*) or TUNEL-positive cells (*G*) per total number of cells taken as 100% and fold changes to control (*H*). Data are means ± SE from three (*E* and *G–I*) and four (*K*) subjects per group. *$P < 0.05$ for LATS1 T1079D versus empty vector (−) (*E* and *G*), LATS1 T1079A and LATS1 kinase-dead (KD) versus empty vector (−) (*I*), and siRNA LATS1 versus control siRNA (−) (*K*) by Mann–Whitney *U* test. WT = wild type.

single amino acid mutation mimicking constitutive T1079 phosphorylation (T1079D) (9), but not WT LATS1, markedly reduced proliferation, increased levels of proapoptotic marker Bim (5), and induced apoptosis (Figures 1E–1G; *see* Figure E3A) without significant effect on cell migration (Figure 1H). Dephosphomimetic LATS1 T1079A, LATS1 KD (9), and siRNA LATS1, but not LATS1 WT and control siRNA, significantly increased proliferation and reduced Bim levels in nondiseased PAVSMCs (Figures 1I–1L; *see* Figures E3B and E3C).

Together, these data demonstrate that LATS1 inactivation caused by T1079 dephosphorylation is required for increased proliferation and survival of human PAH PAVSMCs. Interestingly, T1079A and WT LATS1 down-regulated DNA damage effector poly(ADP-ribose) polymerase1 (PARP1) in human PAH PAVSMCs (17) (*see* Figure E4), suggesting that LATS1-dependent regulation of DNA damage response does not require phosphorylation and is likely uncoupled from LATS1-dependent regulation of proliferation/apoptosis signaling.

HIPPO/LATS1 Inactivation Promotes Human PAH PAVSMC Proliferation and Survival via Yap

We reasoned that LATS1 inactivation in PAH PAVSMCs could result in up-regulation of proproliferative/prosurvival Yap/Taz (21). Indeed, we detected significantly higher Yap/Taz protein levels, activity (Figures 2A–2C), and Yap nuclear accumulation (Figure 2D) in human PAH PAVSMCs compared with control subjects. "Active" LATS1 T1079D, but not WT, significantly reduced Yap/Taz content in human PAH PAVSMCs. Transfection of control PAVSMCs with LATS1 KD or dephosphomimetic LATS1 T1079A markedly increased Yap/Taz protein levels compared with LATS WT-transfected cells (Figures 2E; *see* Figure E5) showing that LATS1 inactivation is responsible for Yap/Taz accumulation. shRNA Yap or verteporfin (VP), a small molecule blocking binding of Yap with its major transcriptional partner TEAD (22), reduced proliferation and promoted apoptosis in human PAH PAVSMCs (Figures 2F–2K). Interestingly, Yap down-regulation significantly decreased Taz levels (Figures 2F and 2I), suggesting a predominant role for Yap versus Taz in regulating PAH PAVSMC proliferative/apoptotic responses.

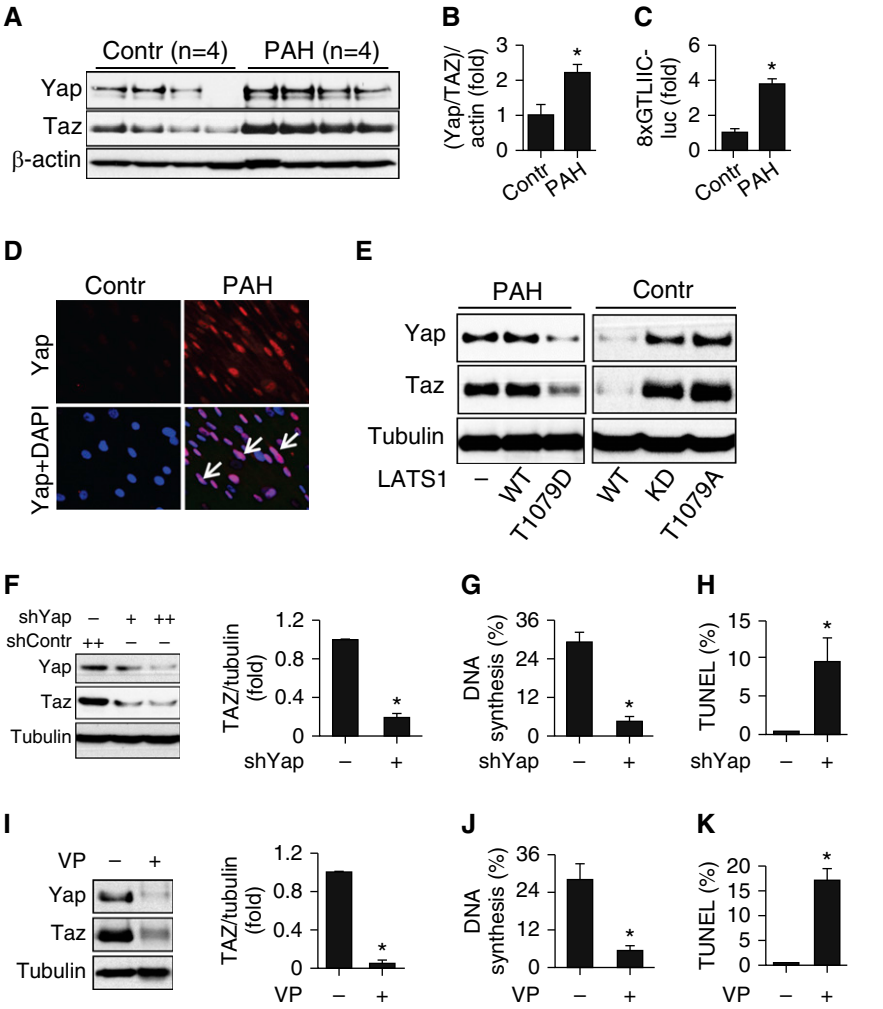

Figure 2. HIPPO/large tumor suppressor 1 (LATS1) inactivation increases human pulmonary arterial hypertension (PAH) pulmonary arterial vascular smooth muscle cell (PAVSMC) proliferation and survival via Yap. (*A* and *B*) Immunoblot analysis of distal PAVSMCs from four nondiseased (control [Contr]) and four subjects with idiopathic PAH; data represent fold changes in Yap/Taz/actin ratio to control; data are means ± SE; four subjects per group; **P* < 0.05 by Mann–Whitney *U* test. (*C*) Endogenous Yap/Taz activity accessed by dual-luciferase reporter assay. Data represent fold changes in 8 × GTIIC-luc/hRluc ratio to control; data are means ± SE; four subjects per group; **P* < 0.05 by Mann–Whitney *U* test. (*D*) Representative images from three subjects per group. Yap, *red*; nuclei (DAPI), *blue*. *Arrows* indicate cells with increased nuclear localization of Yap (*purple*). (*E*) Immunoblot analysis of cells transfected with indicated LATS1 constructs or empty vector (−) for 48 hours. Immunoblots are representative of three separate experiments, each performed on cells from a different subject (*see* Figure E4 for statistical analysis). (*F–K*) Immunoblot (*F* and *I*), DNA synthesis (bromodeoxyuridine [BrdU] incorporation) (*G* and *J*), and apoptosis (terminal deoxynucleotidyl transferase dUTP nick end labeling [TUNEL]) (*H* and *K*) analyses of PAH PAVSMCs infected with shYap-producing or control adenovirus (−) for 72 hours (*F–H*) or treated for 24 hours with 1 μM VP or diluent (−). (*F* and *I*) Data are fold changes in Taz/tubulin ratio to controls; immunoblots are representative of three experiments, each on cells from a different subject with PAH. **P* < 0.05 by Mann–Whitney *U* test. (*G*, *H*, *J*, and *K*) Data represent percentage of BrdU- (*G* and *J*) or TUNEL-positive cells (*H* and *K*) per total number of cells taken as 100%. Data are means ± SE, n = 3 subjects per condition (*F*, *G–I*, and *K*); n = 4 subjects per condition (*J*); **P* < 0.05 by Mann–Whitney *U* test. DAPI = 4′,6-diamidino-2-phenylindole; KD = kinase-dead; sh = short hairpin RNA; VP = verteporfin; WT = wild type.

Bioinformatic analysis (23–26) (*see* online supplement) showed enrichment ($P < 10^{-4}$) of proliferative/survival gene sets AKT, NOTCH, WNT, HIF, and BMP in the shortest paths in a global interactome connecting HIPPO

components to the pulmonary hypertension (PH) network (27) (*see* Figure E6) from which the AKT set was ranked as a most probable candidate. A proliferative/antiapoptotic role of mTOR-Akt and Notch3 intracellular domain in PAH PAVSMCs had been reported by us and others (5, 28, 29), and we confirmed activation of HIF1 and Wnt/β-catenin using respective activation assays (*see* Figure E7). Supporting the bioinformatic predictions, inactivation of LATS1 in nondiseased human PAVSMCs significantly up-regulated mTOR-Akt, as evidenced by increase in P-S473 Akt, mTORC2-specific P-T2481 mTOR, and mTORC1-specific P-S6 (5, 14, 30–32), and led to accumulation of β-catenin, Notch3 intracellular domain, and HIF1α, whereas "restoration" of P-T1079 LATS1 or suppression of Yap in PAH PAVSMCs by LATS1 T1079D or VP had the opposite effect (Figure 3; *see* Figure E8). Collectively, these data show that LATS1 inactivation up-regulates proliferative/prosurvival signaling and promotes human PAH PAVSMC proliferation and survival via Yap.

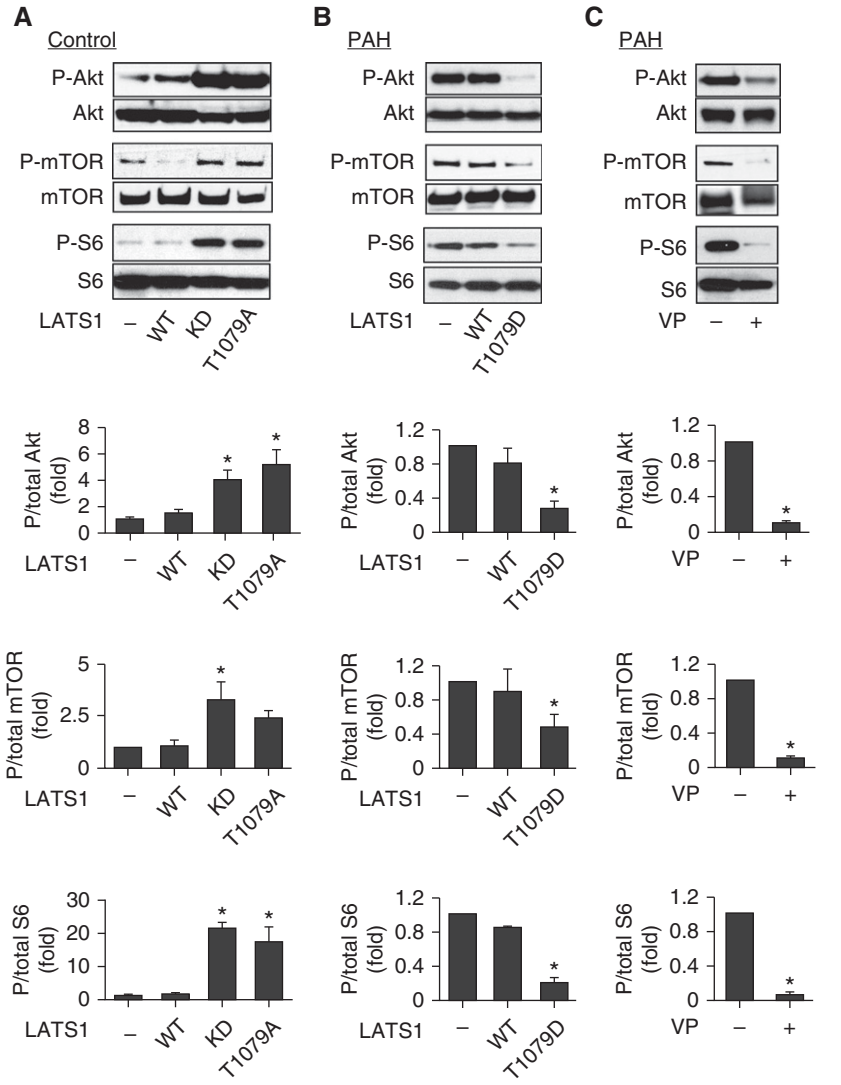

Figure 3. HIPPO/large tumor suppressor 1 (LATS1) inactivation up-regulates mTOR-Akt signaling. Cells were transfected with indicated LATS1 constructs or empty vector (−) (*A* and *B*), or treated with diluent (−) or 1 μM VP for 24 hours (*C*) followed by immunoblot analysis to detect indicated proteins. Representative images and statistical analysis of three separate experiments, each performed on cells from a different subject. Data are fold changes in phospho/total ratios to control (−) (*A* and *B*) or diluent (*C*). Data are means ± SE; *$P < 0.05$ versus − by Mann–Whitney *U* test. KD = kinase-dead; mTOR = mammalian target of rapamycin; PAH = pulmonary arterial hypertension; VP = verteporfin; WT = wild type.

HIPPO/LATS1 Inactivation Promotes Fibronectin Production and Up-regulates Integrin-linked Kinase 1

Because HIPPO/LATS1 inactivation is linked with ECM composition, we next tested whether mechanistic link exists between LATS1 and fibronectin, increased levels of which are linked with pulmonary vascular remodeling (33–35). We found that PAH-derived PAVSMCs produce and secrete higher levels of fibronectin than control subjects (Figures 4A, 4B, 4D, and 4E). LATS1 KD- or LATS1 T1079A-induced HIPPO/LATS inactivation in control PAVSMCs significantly increased fibronectin levels, whereas VP-dependent Yap down-regulation in human PAH PAVSMCs markedly reduced fibronectin content (Figures 4F and 4G). siRNA fibronectin significantly inhibited proliferation and induced apoptosis in PAH PAVSMCs (Figures 4H, 4J, and 4K) showing that LATS1 inactivation and up-regulation of Yap promote fibronectin production that is required for increased PAH PAVSMC proliferation and survival.

The major downstream effector of fibronectin is integrin-linked kinase 1 (ILK1) (36), overexpression of which plays a prooncogenic role in human cancers (37). We found that ILK1 is overexpressed in isolated PAVSMCs and SMA-positive areas of distal remodeled PAs from subjects with idiopathic PAH (Figures 4A and 4L), which was associated with VSM-specific proliferation (PCNA) in remodeled, but not fully obliterated vessels (Figure 4L). Importantly, siRNA fibronectin reduced ILK1 protein levels in human PAH PAVSMCs (Figures 4H and 4I). Furthermore, selective ILK inhibitor Cpd22 (38) suppressed growth, proliferation, and induced apoptosis in human PAH, but not control, PAVSMCs (Figures 5A–5C). In aggregate, these data show that LATS1 inactivation promotes fibronectin production that up-regulates ILK1, leading to increased proliferation and survival of PAH PAVSMCs.

ILK1 Inactivates HIPPO/LATS1 Leading to Increased PAH PAVSMC Proliferation and Survival

To determine the mechanisms of HIPPO/LATS1 inactivation, we first examined LATS1 canonical activators MST1/2, deficiency of which is strongly linked with cancer progression (8). PAH PAVSMCs, although demonstrating

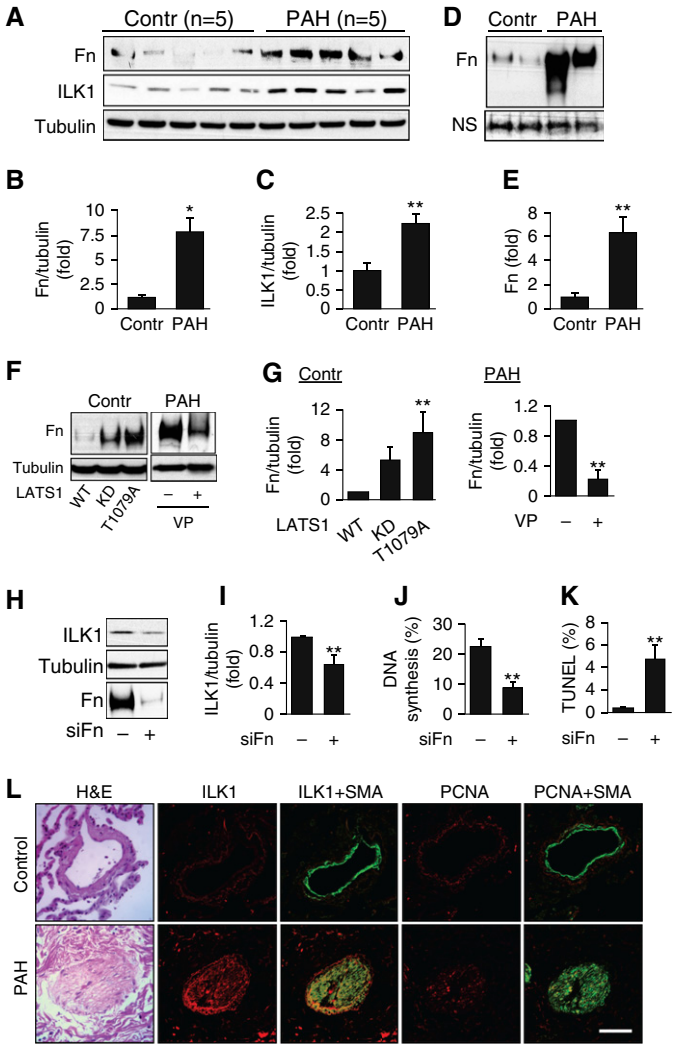

Figure 4. HIPPO/large tumor suppressor 1 (LATS1) inactivation promotes fibronectin production and up-regulates integrin-linked kinase 1 (ILK1). (*A–C*) Immunoblot analysis of distal pulmonary arterial vascular smooth muscle cells from five subjects with idiopathic pulmonary arterial hypertension (PAH) and five nondiseased (control [Contr]) subjects. Data represent fold changes in fibronectin (Fn)/tubulin (*B*) and ILK1/tubulin ratios (*C*) to control subjects. Data are means ± SE; n = 5 subjects per group; $^{*}P < 0.01$, $^{**}P < 0.05$ versus control by Mann–Whitney *U* test. (*D* and *E*) Cells were maintained in cultural media for 48 hours; then supernatants were collected, normalized by total cell protein content, and subjected to immunoblot analysis to assess Fn levels. (*D*) Representative immunoblots. (*E*) Fn protein levels were normalized to the nonsignificant band and presented as fold changes versus control (taken as one fold). Data are means ± SE from n = 4 subjects per group; $^{*}P < 0.05$ versus control by Mann–Whitney *U* test. (*F* and *G*) Cells were transfected with mammalian vectors expressing indicated LATS1 constructs or empty vector (−), or treated with 1 μM VP for 24 hours followed by immunoblot analysis to detect Fn and tubulin. Data are means ± SE from n = 3 subjects per group; data represent fold changes in Fn/tubulin ratio to LATS1 WT or diluent (−), respectively. $^{**}P < 0.05$ by Mann–Whitney *U* test. (*H–K*) PAH pulmonary arterial vascular smooth muscle cells were transfected with small interfering RNA fibronectin (siFn) or control siRNA GLO (−), and immunoblot (*I*), DNA synthesis (bromodeoxyuridine [BrdU]), or apoptosis (terminal deoxynucleotidyl transferase dUTP nick end labeling [TUNEL]) analyses were performed. Data represent ILK1/tubulin ratio folds to control (*I*), percentage of BrdU- (*J*) or TUNEL-positive cells (*K*) per total number of cells taken as 100%. Data are means ± SE from three subjects per group. $^{**}P < 0.05$ versus control siRNA GLO (−) by Mann–Whitney *U* test. (*L*) Histochemical analysis of human lung tissues. *Left to right*: hematoxylin and eosin (H&E) staining; ILK1 (*red*); ILK1 (*red*) + smooth muscle α-actin (SMA) (*green*); proliferating cell nuclear antigen (PCNA) (*red*); PCNA (*red*) + SMA (*green*). Images are representative of three control subjects and three subjects with idiopathic PAH; minimum of 10 PAs per subject. *Scale bar* = 50 μm. KD = kinase-dead; NS = nonspecific; VP = verteporfin; WT = wild type.

P-LATS1 deficiency and Yap/Taz accumulation, showed no reduction of MST1 or MST2 levels and even trend to increased P-T183/T180 MST1/2, contributing to MST activation (*see* Figures E9A–E9F) (8). Furthermore, siRNA-induced knock-down of MST1 or 2 in control PAVSMCs, whereas decreasing MST1/2 levels neither reduced P-T1079 LATS1 nor elevated Yap/Taz (*see* Figure E9G–E9I) suggesting that LATS1 inactivation is likely MST1/2-independent.

To dissect pro-PH factors accounting for PAH-specific HIPPO/LATS1 inactivation in nondiseased PAVSMCs, we first tested substrate stiffness, which can regulate LATS1 in MST-independent manner (39) and was recently reported as an early event inducing Yap/Taz accumulation in PH vasculature (10). We found that maintenance of nondiseased PAVSMCs on the substrates of increased stiffness, reported in PAH PAs, induced P-LATS1 deficiency (Figures 6A and 6B), suggesting the role of increased stiffness in HIPPO/LATS1 inactivation. Because ECM composition and mitogens also regulate the LATS1–Yap/Taz axis in other cell types, we next evaluated various ECM proteins (collagen I, collagen IV, fibronectin, laminin), and soluble pro-PH factors (endothelin receptor 1, interleukin-6, tumor necrosis factor-α, insulin growth factor-1, platelet-derived growth factor-BB [PDGF-BB]) implicated in PAH. Among all tested factors, PDGF-BB and fibronectin induced PAH-specific LATS1-Yap/Taz dysregulation (reduced P-T1079 LATS1 and accumulation of Yap/Taz) (Figures 6C–6G; *see* Figure E10). Together, these data identify PDGF-BB, fibronectin, and increased stiffness as factors inducing HIPPO/LATS1 inactivation and suggest multifactorial mechanism of LATS1-Yap/Taz dysregulation in PAH.

Because all three identified factors activate ILK1, which may act as LATS1 inhibitor in tumor cells (37, 40, 41), we hypothesized that PAH PAVSMC-specific LATS1 inactivation depends on ILK1. We found that Cpd22-mediated ILK inhibition in PAH PAVSMCs increased P-T1079 LATS1; down-regulated Yap/Taz levels, transcriptional activity, and nuclear accumulation; and inhibited LATS1-Yap downstream effectors Akt and mTOR without significant effects on control cells (Figures 5D–5G; *see* Figures E11A and E11B). "Inactive" LATS1 T1079A protected

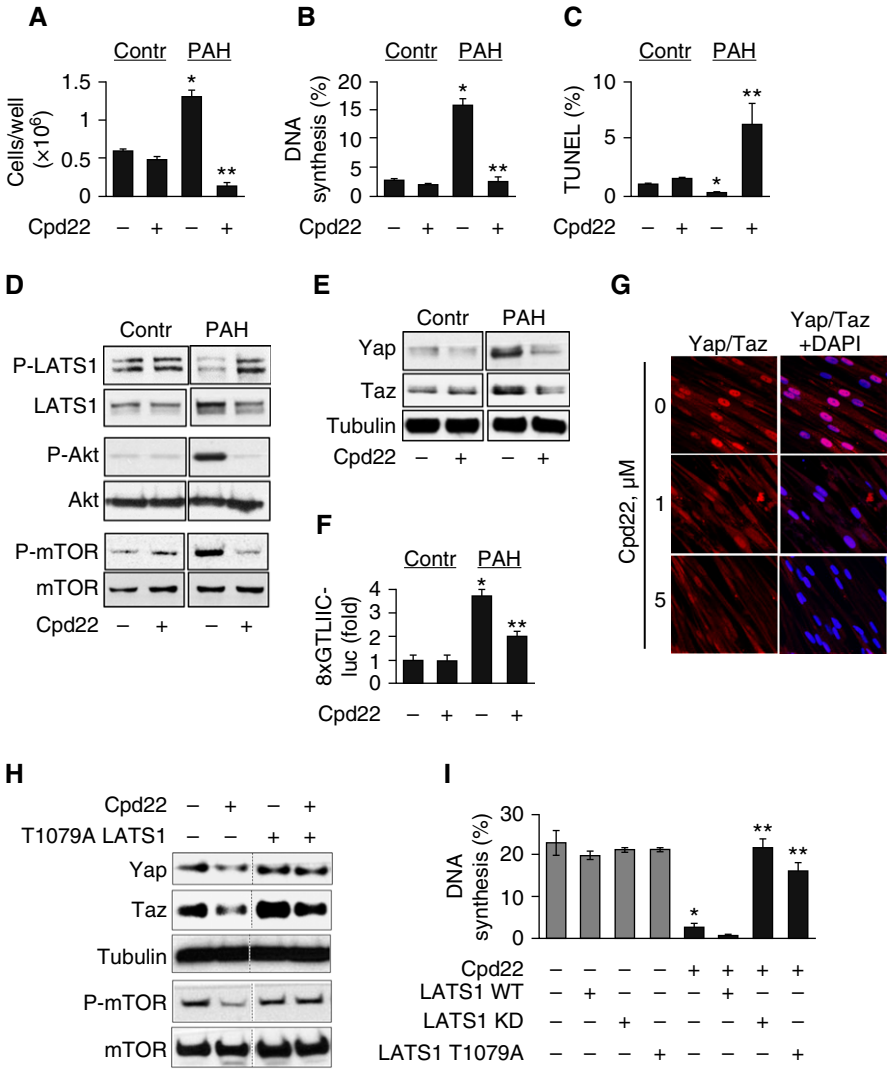

Figure 5. Integrin-linked kinase 1 down-regulates HIPPO/large tumor suppressor 1 (LATS1), leading to increased pulmonary arterial vascular smooth muscle cell (PAVSMC) proliferation and survival. (*A–C*) Cells, treated with diluent (−) or 5 μM Cpd22 were subjected to cell count (5-d treatment) (*A*), DNA synthesis (bromodeoxyuridine, 24-h treatment) (*B*), and apoptosis (TUNEL, 24-h treatment) (*C*) analyses. Data are means ± SE; (*A*) n = 4 subjects per group; (*B* and *C*) n = 3 subjects per group. *$P < 0.05$ for diluent-treated pulmonary arterial hypertension (PAH) versus diluent-treated control (Contr) cells; **$P < 0.05$ for Cpd22- versus diluent-treated PAH PAVSMCs by Mann–Whitney *U* test. (*D* and *E*) Cells were treated with 1 μM Cpd22 for 30 minutes (*D*) or 24 hours (*E*). Immunoblots are representative of three experiments, each performed on cells from a different subject. *See* Figures E11A and E11B for statistical analysis. (*F*) PAH PAVSMCs (four subjects per group), cotransfected with 8 × GTIIC-luc and pGL4 *Renilla* hRluc, were treated with 5μM Cpd22 or diluent (−) (24 h), and endogenous Yap/Taz activity accessed by dual-luciferase reporter assay. *$P < 0.05$ for Contr versus PAH cells; **$P < 0.05$ for diluent- versus Cpd22-treated PAH cells by Mann–Whitney *U* test. (*G*) Immunohistochemical analysis of PAH PAVSMCs treated with indicated concentrations of Cpd22 for 24 hours. *Red*, Yap/Taz; *blue*, DAPI. Images are representative of three separate experiments, each on cells from a different subject. (*H* and *I*) PAH PAVSMCs were transfected with indicated LATS1 constructs or empty vector for 48 hours, treated with 1 μM Cpd22 or diluent (−) for 24 hours, and immunoblot (*H*) or DNA synthesis analyses (*I*) were performed. (*H*) Representative immunoblots from three experiments, each on cells from a separate subject. *See* Figure E11C for statistical analysis. (*I*) *$P < 0.05$ versus empty vector–transfected diluent-treated cells; **$P < 0.05$ versus empty vector-transfected Cpd22-treated cells by Mann–Whitney *U* test. DAPI = 4′,6-diamidino-2-phenylindole; KD = kinase-dead; mTOR = mammalian target of rapamycin; TUNEL = terminal deoxynucleotidyl transferase dUTP nick end labeling; WT = wild type.

PAH PAVSMCs from Cpd22-dependent down-regulation of Yap/Taz and P-2481 mTOR (Figure 5H; *see* Figure E11C). Furthermore, T1079A and KD, but not WT LATS1, prevented Cpd22-dependent inhibition of PAH PAVSMC proliferation (Figure 5I) showing that ILK acts upstream of LATS1.

Together with our findings that LATS1 inactivation up-regulates the fibronectin–ILK1 axis (Figure 4), these data suggest that, in PAH PAVSMCs, LATS1 is self-inactivated via a Yap–fibronectin–ILK1 loop. Confirming our findings, inhibition of ILK with Cpd22 reduced fibronectin levels in PAH PAVSMCs (*see* Figure E12A); and siRNA fibronectin decreased the levels of LATS1 reciprocal effectors Yap/Taz and T2481 mTOR phosphorylation (*see* Figure E12B).

ILK Inhibition Reactivates HIPPO/LATS1, Reduces Established Pulmonary Vascular Remodeling and PH, and Improves RV Morphology and Function *In Vivo*

Rats with SU5416/hypoxia-induced PH (18, 20, 42) showed decreased P-T1079 LATS1, overexpression of ILK1, and increased proliferation (detected by PCNA) in SMA-positive areas of small (25–150 μm) remodeled PAs (Figure 7A) suggesting that the signaling abnormalities with human PAH are shared. Reduced P-T1079 LATS1 was also detected in RV, but not skeletal muscle from rat PH cohort (*see* Figure E13), suggesting potential link between LATS1 down-regulation and RV dysfunction.

Following our *in vitro* findings, we tested effects of Cpd22 on established PH *in vivo* (*see* Figure E15). Three weeks after SU5416/hypoxia challenge, similar to human PAH (Figure 4L), small remodeled PAs from animals with SU5416/hypoxia-induced PH showed P-T1079 LATS1 reduction and overexpression of ILK1 (Figure 7B), suggesting that signaling mechanisms with human PAH are shared. That was associated with significant VSM remodeling, elevated RV systolic and mean PA (sRVP and mPAP) pressures without significant changes in systolic left ventricular pressure and mean arterial pressure, increased total pulmonary vascular resistance, RV hypertrophy, and max dP/dT (Figures 7C–7H; *see* Figure E14), indicative of a developed PH phenotype. Starting Day 22, mice, still kept

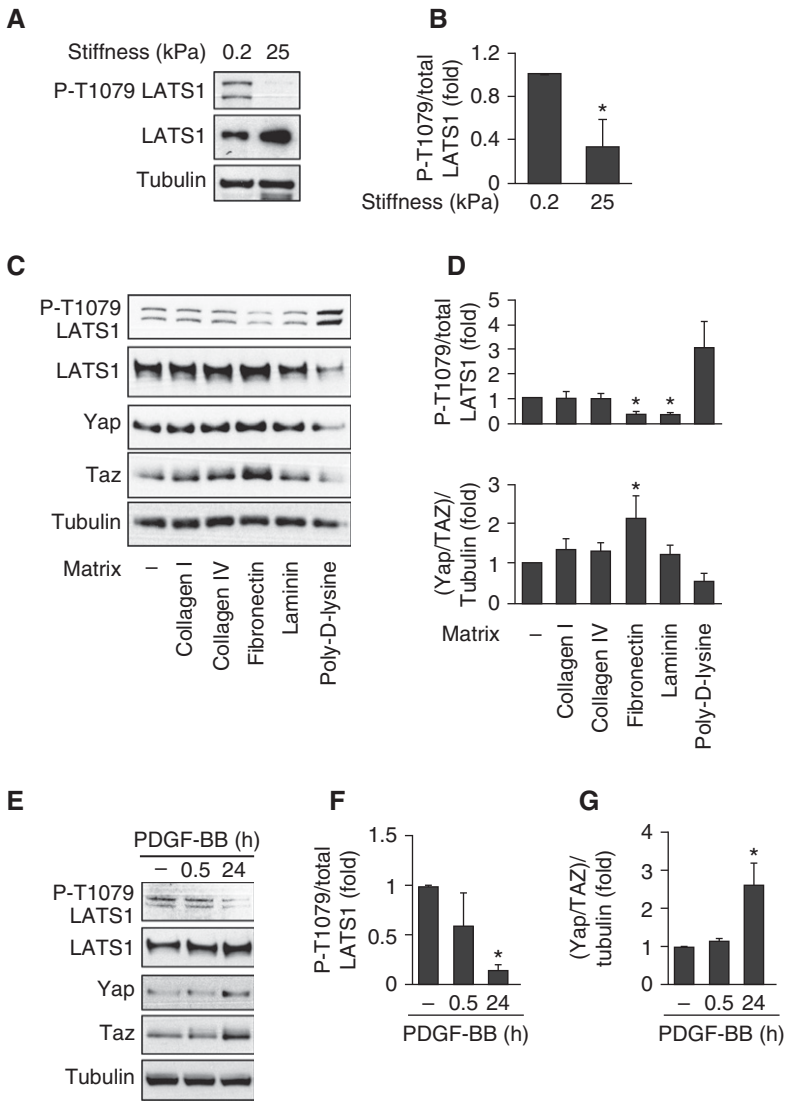

Figure 6. Increased substrate stiffness, fibronectin, and platelet-derived growth factor-BB (PDGF-BB) down-regulate HIPPO/large tumor suppressor 1 (LATS1) signaling in nondiseased pulmonary arterial vascular smooth muscle cells. (*A–G*) Immunoblot analysis of nondiseased (control) human pulmonary arterial vascular smooth muscle cells maintained on the Softwell hydrogels with 0.2-kPa and 25-kPa stiffness (*A* and *B*), plates covered with indicated matrix proteins (*C* and *D*), or treated with 10 ng/ml PDGF-BB for 0.5 and 24 hours (*E–G*; *see* Figure E10 for IL-6, ET-1, tumor necrosis factor-α, and insulin-like growth factor-1). Immunoblots are representative of three separate experiments, each performed on cells from a different subject. Data are means ± SE from three subjects per group; *$P < 0.05$ versus control (−) (*B*, *F*, and *G*); *$P < 0.05$ versus control and versus poly-D-lysine (*D*) by Mann–Whitney *U* test.

under hypoxia, were randomly assigned to two groups and treated with Cpd22 or vehicle for 2 weeks. Vehicle-treated animals showed the trend to phenotype worsening (further increase in sRVP and VSM remodeling) compared with the 3-week time-point. Cpd22 restored P-T1079 LATS1 in SMA-positive areas in small muscular PAs, reduced VSM remodeling, and decreased sRVP and mPAP without significant effects on systolic left ventricular pressure and mean arterial pressure (Figures 8A–8D; *see* Figure E16). Cpd22-treated mice showed decreased RV hypertrophy and improved max dP/dT (Figures 8F and 8E, respectively) and RV contractile index (98.7 + 3.7 vs. 81.8 + 3.7 in vehicle-treated mice; $P < 0.05$) suggesting that Cpd22 improves RV morphology and function. Collectively, these data demonstrate that ILK inhibition restores LATS1 signaling and reverses established pulmonary vascular remodeling and PH *in vivo*.

Discussion

This study identifies HIPPO/LATS1 signaling as an important regulator of proliferative apoptosis-resistant PAVSMC phenotype in PAH and suggests a potentially attractive therapeutic target pathway to reduce existing pulmonary vascular remodeling and PH (Figure 8G). Our new findings include that (*1*) HIPPO/LATS1 is inactivated in distal remodeled PA from subjects with idiopathic PAH and two rodent models of severe PH, and in human PAH PAVSMCs; (*2*) LATS1 inactivation enables activation of Yap, consequent up-regulation of proproliferative/prosurvival pathways, and increased proliferation and survival; (*3*) LATS1 inactivation is self-supported by bidirectional negative cross-talk with ILK1 via the Yap–fibronectin axis; and (*4*) pharmacologic inhibition of ILK up-regulates LATS1, inhibits proliferation, and induces apoptosis in human PAH, but not control PAVSMCs, and reduces established pulmonary vascular remodeling and PH *in vivo*.

Defective coordination of cell death and proliferation in microvascular PAVSMCs underlines pulmonary vascular remodeling, a critical component of PAH. Here, we demonstrate that HIPPO signaling, a nexus of proliferation/apoptosis balance (21), is disrupted in the proliferative PAVSMCs from small remodeled PAs in idiopathic PAH lungs, evidenced by the deficiency of the active phosphorylated form of its core growth-suppressor kinase LATS1, which is coupled with up-regulation of its major reciprocal effectors Yap/Taz, stimulators of proliferation, survival, and self-renewal (21, 43). Using a panel of LATS1 mutants, bioinformatic network-based approach, and siRNA and pharmacologic interventions, we found that active LATS1 maintains low proliferation rates and physiologic levels of apoptosis in adult PAVSMCs, whereas its inactivation promotes concomitant activation of Yap, up-regulation of several proliferative/prosurvival signaling pathways without the need of stimulating it cognate receptors, and acquisition of a proliferative, apoptosis-resistant PAVSMC phenotype.

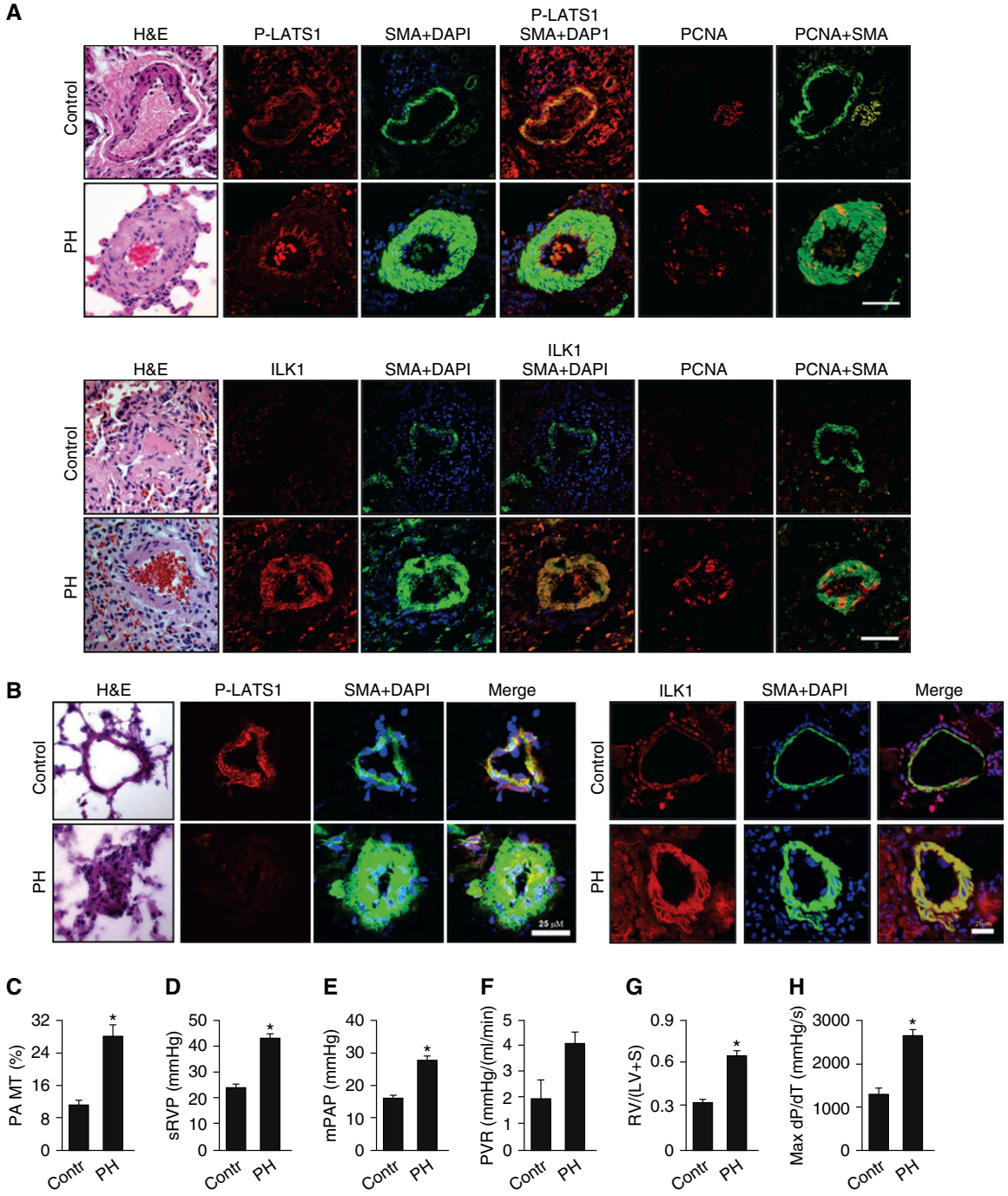

Figure 7. P-T1079 large tumor suppressor 1 (Lats1) deficiency in murine animal models of pulmonary hypertension (PH). (*A*) Hematoxylin and eosin (H&E) and immunohistochemical analyses of lung tissues from 6- to-8-week-old male Sprague-Dawley rats with SU5416/hypoxia-induced PH (8 wk of PH induction). *Upper panel (left to right)*: H&E staining; P-T1079 LATS1 (*red*); smooth muscle α-actin (SMA) (*green*) + 4′,6-diamidino-2-phenylindole (DAPI) (*blue*); P-T1079 LATS1 (*red*) + SMA (*green*) + DAPI (*blue*); proliferating cell nuclear antigen (PCNA) (*red*); PCNA (*red*) + SMA (*green*). *Lower panel (left to right)*: H&E staining; integrin-linked kinase 1 (ILK1) (*red*); SMA (*green*) + DAPI (*blue*); ILK1 (*red*) + SMA (*green*) + DAPI (*blue*); PCNA (*red*); PCNA (*red*) + SMA (*green*). Images are representative of three animals per condition, minimum of 10 vessels per animal per condition. *Scale bar* = 50 μm. (*B*) H&E staining and immunohistochemical analysis of lung tissues from 6- to-8-week-old C57BL/6J mice with SU5416/hypoxia-induced PH (3 wk of PH induction). Images are representative of three animals per condition, 10 pulmonary arteries (PAs) per animal per condition. *Red*, P-T1079 Lats1 (*left panel*) and ILK1 (*right panel*); *green*, SMA; *blue*, DAPI. *Scale bar* = 25 μm. (*C–F*) PA medial thickness (MT) (*C*), mean systolic right ventricular pressure (sRVP) (*D*), mean pulmonary artery pressure (mPAP) (*E*), total pulmonary vascular resistance (PVR) (*F*), Fulton index (RV/[LV + S]) (*G*), and max dP/dT (*H*) of mice subjected to SU5416/hypoxia or normoxia exposure for 3 weeks. n = 5 mice/control (Contr) group; n = 6 mice per PH group. Data are means ± SE; **P* < 0.01 by Mann–Whitney *U* test. *See* Figure E14 for systolic left ventricular pressure and mean arterial pressure data. LV = left ventricle; RV = right ventricle; S = septum.

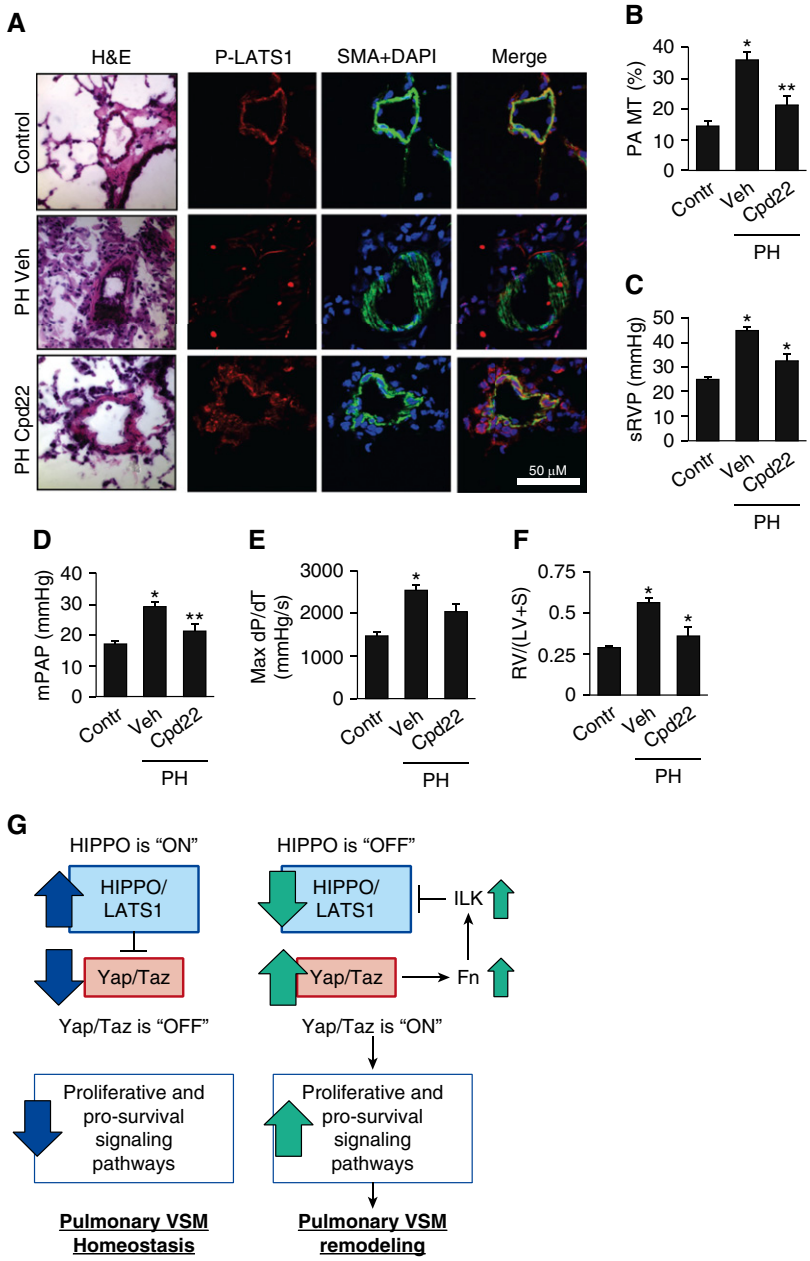

Figure 8. (*A–F*) Cpd22 reactivates large tumor suppressor 1 (Lats1), reduces established pulmonary vascular remodeling and pulmonary hypertension (PH). Six- to 8-week-old male C57BL/6J mice were subjected to SU5416/hypoxia exposure as described in the METHODS section. Three weeks after PH induction, mice were treated with vehicle (Veh) or Cpd22 (20 mg/kg, intraperitoneally, 5 d/wk) for 2 weeks. Then hemodynamic measurements were performed, lung and heart tissues were collected for immunohistochemical and morphologic analyses; Fulton index was calculated as RV/(LV + S) ratio. Normoxia-maintained same-age male C57BL/6J mice were used as control (Contr) animals. (*A*) Hematoxylin and eosin (H&E) staining and immunohistochemical analysis of lung tissue sections. Images were representative of three mice per condition; minimum of 10 pulmonary arteries (PAs) per condition. *Red*, P-T1079 Lats1; *green*, smooth muscle α-actin (SMA); *blue*, DAPI. *Scale bar* = 50 μm. (*B–F*) PA medial thickness (MT) (*B*), systolic right ventricular pressure (sRVP) (*C*), mean pulmonary arterial pressure (mPAP) (*D*), max dP/dT (*E*), and Fulton index (*F*). Data are means ± SE; n = 5–8 mice per group. $^{*}P < 0.01$ for PH Veh versus Contr (*B–F*) and for PH Cpd22 versus PH Veh (*D*); $^{**}P < 0.05$ for PH Cpd22 versus PH Veh (*B* and *C*) by Mann–Whitney *U* test (see Figure E16 for systolic left ventricular pressure and mean arterial pressure). (*G*) Schematic representation of the potential function of HIPPO in nondiseased pulmonary arterial vascular smooth muscle cells (VSM) (*left*) and proposed mechanism of pulmonary VSM-specific HIPPO dysfunction in PH (*right*). DAPI = 4′,6-diamidino-2-phenylindole; Fn = fibronectin; ILK = integrin-linked kinase; LV = left ventricle; RV = right ventricle; S = septum.

The postulated key role for LATS1 in unstimulated proliferation and survival of PAH PAVSMCs is further supported by our new findings showing that LATS1 dysfunction is self-preserved by a pathogenic loop via Yap/fibronectin-dependent up-regulation of ILK1, which inhibits LATS1 and "locks" HIPPO in an inactive state (Figure 8G) that can explain increased proliferation and apoptosis resistance of PAH PAVSMCs without mitogenic stimuli.

Although elevated levels of fibronectin in remodeled PAs in PAH have been positively associated with medial hypertrophy and neointima formation (33–35), its role in the proliferative response of pulmonary vascular cells in PAH remained unclear. We demonstrate that PAH-specific dysregulation of LATS1-Yap in PAVSMCs promotes fibronectin production, which is required for increased proliferation and survival. This observation is suggestive of PAVSMC involvement in modulating ECM composition and provides a functional link between fibronectin and proliferative/prosurvival PAVSMC phenotype in PAH.

Moreover, we found that increased fibronectin content in human PAH PAVSMCs supports overexpression of ILK1, a LATS1 inhibitor in tumor cells (40). Although never studied in PAH, fibronectin-induced ILK1 overexpression in human cancers promotes cell proliferation and survival with or without growth factor receptor involvement (37). We found that selective ILK inhibition reactivates HIPPO/LATS1 in PAH PAVSMCs, leading to down-regulation of LATS1 reciprocal downstream effectors Yap/Taz and mTOR, suppression of proliferation, and induction of apoptosis. To our knowledge, these data present the first evidence of a bidirectional negative cross-talk between LATS1 and ILK1, which provides a novel mechanistic link between ECM remodeling and increased proliferation and survival of PAVSMCs in PAH.

Our findings suggest a multifactorial nature of LATS1 down-regulation by increased stiffness, fibronectin, and promitogenic PDGF-BB. Supporting our observations, increased stiffness was recently reported as an early event inducing adventitial fibroblasts-specific Yap/Taz in PH (10), but the links among ECM, PDGF, and HIPPO/LATS1 remain to be elucidated. We also anticipate that other

factors, such as dysregulation of BMPRII and transforming growth factor-β signaling, linked with HIPPO and Yap in cancer and embryonic stem cells (21, 44–46), might further impact LATS1-dependent regulation of PAVSMC phenotype in PAH. Furthermore, HIPPO/LATS1 involvement in PAH may not be restricted by pulmonary vasculature. Indeed, LATS1 down-regulation in RV from rats with experimental PH raises the possibility of HIPPO/LATS1 involvement in RV hypertrophy and/or dysfunction, which is shown to be linked with fibrosis and abnormal ECM content.

Collectively, our study demonstrates a key role for LATS1-ILK1 cross-talk in the increased proliferation and survival of PAVSMCs in PAH. Attractiveness of this pathway as a potential therapeutic target is further supported by our observations that pharmacologic disruption of this pathogenic loop by Cpd22 does not restore nondiseased cell phenotype, but selectively eliminates diseased cells via induction of apoptosis. ILK1 inhibitors have shown great potential in preclinical cancer studies as highly selective agents without apparent toxicity and currently are under development for clinical use or entered clinical trials (38, 47–49). Although our study has focused on the PAVSMCs and not other pulmonary vascular cell types, adventitial fibroblasts and endothelial cells in human PAH also have proliferation/apoptosis imbalance, suggesting potential involvement of HIPPO and/or ILK1. Given our current findings that Cpd22 reduces established PH *in vivo*, preclinical testing of ILK inhibitors on other human PAH cell types and experimental PH models warrants further investigation. ■

Author disclosures are available with the text of this article at www.atsjournals.org.

References

1. Humbert M, Morrell NW, Archer SL, Stenmark KR, MacLean MR, Lang IM, Christman BW, Weir EK, Eickelberg O, Voelkel NF, *et al*. Cellular and molecular pathobiology of pulmonary arterial hypertension. *J Am Coll Cardiol* 2004;43(Suppl. S):13S–24S.
2. Morrell NW, Adnot S, Archer SL, Dupuis J, Jones PL, MacLean MR, McMurtry IF, Stenmark KR, Thistlethwaite PA, Weissmann N, *et al*. Cellular and molecular basis of pulmonary arterial hypertension. *J Am Coll Cardiol* 2009;54(Suppl. 1)S20–S31.
3. Erzurum S, Rounds SI, Stevens T, Aldred M, Aliotta J, Archer SL, Asosingh K, Balaban R, Bauer N, Bhattacharya J, *et al*. Strategic plan for lung vascular research: an NHLBI-ORDR Workshop Report. *Am J Respir Crit Care Med* 2010;182:1554–1562.
4. de Jesus Perez V, Yuan K, Alastalo T-P, Spiekerkoetter E, Rabinovitch M. Targeting the Wnt signaling pathways in pulmonary arterial hypertension. *Drug Discov Today* 2014;19:1270–1276.
5. Goncharov DA, Kudryashova TV, Ziai H, Ihida-Stansbury K, DeLisser H, Krymskaya VP, Tuder RM, Kawut SM, Goncharova EA. Mammalian target of rapamycin complex 2 (mTORC2) coordinates pulmonary artery smooth muscle cell metabolism, proliferation, and survival in pulmonary arterial hypertension. *Circulation* 2014;129:864–874.
6. Rabinovitch M. Molecular pathogenesis of pulmonary arterial hypertension. *J Clin Invest* 2012;122:4306–4313.
7. West JD, Austin ED, Gaskill C, Marriott S, Baskir R, Bilousova G, Jean J-C, Hemnes AR, Menon S, Bloodworth NC, *et al*. Identification of a common Wnt-associated genetic signature across multiple cell types in pulmonary arterial hypertension. *Am J Physiol Cell Physiol* 2014; 307:C415–C430.
8. Johnson R, Halder G. The two faces of Hippo: targeting the HIPPO pathway for regenerative medicine and cancer treatment. *Nat Rev Drug Discov* 2014;13:63–79.
9. Chan EHY, Nousiainen M, Chalamalasetty RB, Schafer A, Nigg EA, Sillje HHW. The Ste20-like kinase Mst2 activates the human large tumor suppressor kinase Lats1. *Oncogene* 2005;24:2076–2086.
10. Bertero T, Cottrill KA, Lu Y, Haeger CM, Dieffenbach P, Annis S, Hale A, Bhat B, Kaimal V, Zhang YY, *et al*. Matrix remodeling promotes pulmonary hypertension through feedback mechanoactivation of the YAP/TAZ-miR-130/301 circuit. *Cell Reports* 2015;13: 1016–1032.
11. Guignabert C, Tu L, Le Hiress M, Ricard N, Sattler C, Seferian A, Huertas A, Humbert M, Montani D. Pathogenesis of pulmonary arterial hypertension: lessons from cancer. *Eur Respir Rev* 2013;22:543–551.
12. Schermuly RT, Ghofrani HA, Wilkins MR, Grimminger F. Mechanisms of disease: pulmonary arterial hypertension. *Nat Rev Cardiol* 2011;8: 443–455.
13. Rappaport N, Nativ N, Stelzer G, Twik M, Guan-Golan Y, Iny Stein T, Bahir I, Belinky F, Morrey CP, Safran M, *et al*. MalaCards: an integrated compendium for diseases and their annotation. *Database* 2013;2013:1–14.
14. Krymskaya VP, Snow J, Cesarone G, Khavin I, Goncharov DA, Lim PN, Veasey SC, Ihida-Stansbury K, Jones PL, Goncharova EA. mTOR is required for pulmonary arterial vascular smooth muscle cell proliferation under chronic hypoxia. *FASEB J* 2011;25:1922–1933.
15. Goncharova EA, Goncharov DA, Krymskaya VP. Assays for in vitro monitoring of human airway smooth muscle (ASM) and human pulmonary arterial vascular smooth muscle (VSM) cell migration. *Nat Protoc* 2006;1:2933–2939.
16. Dupont S, Morsut L, Aragona M, Enzo E, Giulitti S, Cordenonsi M, Zanconato F, Le Digabel J, Forcato M, Bicciato S, *et al*. Role of YAP/TAZ in mechanotransduction. *Nature* 2011;474:179–183.
17. Meloche J, Pflieger A, Vaillancourt M, Paulin R, Potus F, Zervopoulos S, Graydon C, Courboulin A, Breuils-Bonnet S, Tremblay E, *et al*. Role for DNA damage signaling in pulmonary arterial hypertension. *Circulation* 2014;129:786–797.
18. Taraseviciene-Stewart L, Kasahara Y, Alger L, Hirth P, Mc Mahon G, Waltenberger J, Voelkel NF, Tuder RM. Inhibition of the VEGF receptor 2 combined with chronic hypoxia causes cell death-dependent pulmonary endothelial cell proliferation and severe pulmonary hypertension. *FASEB J* 2001;15:427–438.
19. Kelley EE, Baust J, Bonacci G, Golin-Bisello F, Devlin JE, St Croix CM, Watkins SC, Gor S, Cantu-Medellin N, Weidert ER, *et al*. Fatty acid nitroalkenes ameliorate glucose intolerance and pulmonary hypertension in high-fat diet-induced obesity. *Cardiovasc Res* 2014;101:352–363.
20. Vitali SH, Hansmann G, Rose C, Fernandez-Gonzalez A, Scheid A, Mitsialis SA, Kourembanas S. The Sugen 5416/hypoxia mouse model of pulmonary hypertension revisited: long-term follow-up. *Pulm Circ* 2014;4:619–629.
21. Gomez M, Gomez V, Hergovich A. The HIPPO pathway in disease and therapy: cancer and beyond. *Clin Transl Med* 2014;3:22.
22. Liu-Chittenden Y, Huang B, Shim JS, Chen Q, Lee S-J, Anders RA, Liu JO, Pan D. Genetic and pharmacological disruption of the TEAD-YAP complex suppresses the oncogenic activity of YAP. *Genes Dev* 2012;26:1300–1305.
23. Igarashi Y, Eroshkin A, Gramatikova S, Gramatikoff K, Zhang Y, Smith JW, Osterman AL, Godzik A. CutDB: a proteolytic event database. *Nucleic Acids Res* 2007;35:D546–D549.
24. Dinkel H, Chica C, Via A, Gould CM, Jensen LJ, Gibson TJ, Diella F. Phospho.ELM: a database of phosphorylation sites—update 2011. *Nucleic Acids Res* 2011;39:D261–D267.
25. Orchard S, Ammari M, Aranda B, Breuza L, Briganti L, Broackes-Carter F, Campbell NH, Chavali G, Chen C, del-Toro N, *et al*. The MIntAct project–IntAct as a common curation platform for 11 molecular interaction databases. *Nucleic Acids Res* 2014;42:D358–D363.
26. Rual J-F, Venkatesan K, Hao T, Hirozane-Kishikawa T, Dricot A, Li N, Berriz GF, Gibbons FD, Dreze M, Ayivi-Guedehoussou N, *et al*. Towards a proteome-scale map of the human protein-protein interaction network. *Nature* 2005;437:1173–1178.
27. Bertero T, Lu Y, Annis S, Hale A, Bhat B, Saggar R, Saggar R, Wallace WD, Ross DJ, Vargas SO, *et al*. Systems-level regulation of microRNA networks by miR-130/301 promotes pulmonary hypertension. *J Clin Invest* 2014;124:3514–3528.

28. Tang H, Chen J, Fraidenburg DR, Song S, Sysol JR, Drennan AR, Offermanns S, Ye RD, Bonini MG, Minshall RD, *et al*. Deficiency of Akt1, but not Akt2, attenuates the development of pulmonary hypertension. *Am J Physiol Lung Cell Mol Physiol* 2015;308:L208–L220.
29. Li X, Zhang X, Leathers R, Makino A, Huang C, Parsa P, Macias J, Yuan JXJ, Jamieson SW, Thistlethwaite PA. Notch3 signaling promotes the development of pulmonary arterial hypertension. *Nat Med* 2009; 15:1289–1297.
30. Goncharova EA, Goncharov DA, Li H, Pimtong W, Lu S, Khavin I, Krymskaya VP. mTORC2 is required for proliferation and survival of TSC2-null cells. *Mol Cell Biol* 2011;31:2484–2498.
31. Guertin DA, Stevens DM, Thoreen CC, Burds AA, Kalaany NY, Moffat J, Brown M, Fitzgerald KJ, Sabatini DM. Ablation in mice of the mTORC components raptor, rictor, or mLST8 reveals that mTORC2 is required for signaling to Akt-FOXO and PKCα, but not S6K1. *Dev Cell* 2006;11:859–871.
32. Sarbassov DD, Guertin DA, Ali SM, Sabatini DM. Phosphorylation and regulation of Akt/PKB by the rictor-mTOR complex. *Science* 2005; 307:1098–1101.
33. Gagné D, Groulx J-F, Benoit YD, Basora N, Herring E, Vachon PH, Beaulieu J-F. Integrin-linked kinase regulates migration and proliferation of human intestinal cells under a fibronectin-dependent mechanism. *J Cell Physiol* 2010;222:387–400.
34. Jones PL, Cowan KN, Rabinovitch M. Tenascin-C, proliferation and subendothelial fibronectin in progressive pulmonary vascular disease. *Am J Pathol* 1997;150:1349–1360.
35. Mitani Y, Ueda M, Komatsu R, Maruyama K, Nagai R, Matsumura M, Sakurai M. Vascular smooth muscle cell phenotypes in primary pulmonary hypertension. *Eur Respir J* 2001;17:316–320.
36. Wu C, Dedhar S. Integrin-linked kinase (ILK) and its interactors: a new paradigm for the coupling of extracellular matrix to actin cytoskeleton and signaling complexes. *J Cell Biol* 2001;155:505–510.
37. McDonald PC, Fielding AB, Dedhar S. Integrin-linked kinase: essential roles in physiology and cancer biology. *J Cell Sci* 2008;121:3121–3132.
38. Lee S-L, Hsu E-C, Chou C-C, Chuang H-C, Bai L-Y, Kulp SK, Chen C-S. Identification and characterization of a novel integrin-linked kinase inhibitor. *J Med Chem* 2011;54:6364–6374.
39. Morgan JT, Murphy CJ, Russell P. What do mechanotransduction, Hippo, Wnt, and TGFβ have in common? YAP and TAZ as key orchestrating molecules in ocular health and disease. *Exp Eye Res* 2013;115:1–12.
40. Serrano I, McDonald PC, Lock F, Muller WJ, Dedhar S. Inactivation of the Hippo tumour suppressor pathway by integrin-linked kinase. *Nat Commun* 2013;4:2976.
41. Shkumatov A, Thompson M, Choi KM, Sicard D, Baek K, Kim DH, Tschumperlin DJ, Prakash YS, Kong H. Matrix stiffness-modulated proliferation and secretory function of the airway smooth muscle cells. *Am J Physiol Lung Cell Mol Physiol* 2015;308: L1125–L1135.
42. Ciuclan L, Bonneau O, Hussey M, Duggan N, Holmes AM, Good R, Stringer R, Jones P, Morrell NW, Jarai G, *et al*. A novel murine model of severe pulmonary arterial hypertension. *Am J Respir Crit Care Med* 2011;184:1171–1182.
43. Harvey KF, Zhang X, Thomas DM. The HIPPO pathway and human cancer. *Nat Rev Cancer* 2013;13:246–257.
44. Varelas X, Samavarchi-Tehrani P, Narimatsu M, Weiss A, Cockburn K, Larsen BG, Rossant J, Wrana JL. The Crumbs complex couples cell density sensing to HIPPO-dependent control of the TGF-β-SMAD pathway. *Dev Cell* 2010;19:831–844.
45. Varelas X, Sakuma R, Samavarchi-Tehrani P, Peerani R, Rao BM, Dembowy J, Yaffe MB, Zandstra PW, Wrana JL. TAZ controls Smad nucleocytoplasmic shuttling and regulates human embryonic stem-cell self-renewal. *Nat Cell Biol* 2008;10:837–848.
46. Nishio M, Otsubo K, Maehama T, Mimori K, Suzuki A. Capturing the mammalian HIPPO: elucidating its role in cancer. *Cancer Sci* 2013; 104:1271–1277.
47. Liu J, Costello PC, Pham NA, Pintillie M, Jabali M, Sanghera J, Tsao MS, Johnston MR. Integrin-linked kinase inhibitor KP-392 demonstrates clinical benefits in an orthotopic human non-small cell lung cancer model. *J Thorac Oncol* 2006;1:771–779.
48. Edwards LA, Thiessen B, Dragowska WH, Daynard T, Bally MB, Dedhar S. Inhibition of ILK in PTEN-mutant human glioblastomas inhibits PKB/Akt activation, induces apoptosis, and delays tumor growth. *Oncogene* 2005;24:3596–3605.
49. Mikalsen T, Gertis N, Moens U. Inhibitors of signal transduction protein kinases as targets for cancer therapy. In: Raafat El-Gewely M, editor. Biotechnology annual review. Amsterdam, the Netherlands: Elsevier Science; 2006. pp. 153–224.
50. Akhmedov NB, Yamashita CK, Tran D, Piri NI, Aguirre GD, Farber DB. Two forms of the large tumor suppressor gene (Lats1) protein expressed in the vertebrate retina. Biochim Biophys Acta Gene Struct Expression 2005;1728:11–17.